

Effect of ultrasonic distillation on performance parameters of seawater desalination and optimization of performance ratio

Jitian Song*, Xu Liu*, Dongqi Shi, Shanlin Zhou, Hang Su, Xiaoxu Bi, Kaijie Cai, Wei Tian

Tianjin University of Science and Technology, Tianjin 300222, China, emails: songjt@tust.edu.cn (J.T. Song), landm511@163.com (X. Liu), 975407468@qq.com (D.Q. Shi), 1569482457@qq.com, (S.L. Zhou), wiewei6375@163.com (H. Sui), 1025393255@qq.com (X.X. Bi), 1543265268@qq.com (K.J. Cai), weitian@tust.edu.cn (W. Tian)

Received 13 January 2022; Accepted 2 June 2022

ABSTRACT

In seawater desalination, the conventional central circulation tube evaporator frequently suffers from insufficient heat transfer and low evaporation efficiency. To measure the effectiveness of seawater desalination, this study incorporates an ultrasonic wave into the typical evaporation process and measures the performance ratio and the specific heat transfer area of the evaporator. Using an ultrasonic evaporator instead of a regular one can enhance the performance ratio from 5.31% to 11.81% while decreasing the specific heat transfer area from 8.70% to 17.01%. On the basis of single factor test, Minitab17 software was utilized to conduct the response surface test of seawater desalination process with four factors and three levels, the optimal performance ratio procedure after optimization is as follows: evaporation temperature 80°C, feed temperature 85°C, feed flow of 50 kg/h, ultrasonic power density is 1.0 W/cm², performance ratio can reach a maximum 0.832 at this time.

Keywords: Performance ratio; Specific heat transfer area of evaporator; Ultrasonic; Response surface analysis

1. Introduction

Seawater desalination technology has undergone decades of continuous development and reform, and it now exhibits unique development tendencies in terms of technology, scale, and application. A wide range of desalination technologies have been developed during the past few decades, including distillation, electrodialysis, reverse osmosis, and more. At present, some new technologies have been used for seawater desalination, such as using microfiltration membranes [1] and solar energy [2]. Seawater desalination is becoming more affordable, and in some nations and locations, the volume of seawater desalination is sufficient to meet the needs of cities' water supply. The use of distillation for seawater desalination accounts for approximately 55 percent of the world's total seawater desalination capacity. However, this seawater desalination technology is plagued by numerous issues, the most significant of which

is its high energy consumption, which results in high production costs; secondly, the seawater desalination plant will incur a massive cost burden due to considerations such as heat exchange area [3]. Studies show that adding an ultrasonic wave into traditional evaporator can greatly improve the heat transfer efficiency [4], thus improving the performance of evaporator.

Trushlyakov et al. [5] evaluated the influence of ultrasonic and pressure on evaporation temperature in a vacuum chamber under the condition of ultrasonic frequency of 25 kHz and ultrasonic vibration amplitude of 2 μm. In our experiment, we found that the liquid temperature rose suddenly from 27.7°C to 32.8°C at the beginning, and then gradually decreased after 45 kPa pressure was reached in the vacuum chamber, until an ice crust was formed on the liquid surface. In cavitation bubbles forming on the surface of the liquid there is an 8% difference in temperature between the initial moment and the moment of cavitation

* Corresponding authors.

bubble formation. Ghafurian et al. [6] studied the effect of ultrasonic time on the evaporation rate of seawater containing minicomputer (a mixture of multi-walled carbon nanotubes and graphene nanoplates). The results demonstrate that when evaporation is 0.01%, solar illumination is 3.6 times and evaporation time is 120 min, the evaporation efficiency reaches the highest 61.3%. Dehbani and Rahimi [7] studied the evaporation rate of NaCl solution in fall-film evaporator after the addition of ultrasonic wave, and the results showed that cavitation bubbles generated at different temperatures had diverse effects on the evaporation rate. At low temperature, ultrasound increases the evaporation rate, while at elevated temperature, evaporation rate is reduced due to a large number of bubbles connected to cover the surface of the plate. When the Reynolds number reaches 250, the evaporation rate increases by 353%. Song et al. [8] studied the heat transfer performance of ultrasonic evaporator by taking tap water as the research object. It needs to be shown that, as the ultrasonic power density increases, the heat transfer coefficient increases before declining. In the presence of ultrasonic, the heat transfer coefficient increases by 17.06%–29.85% more than in the absence of ultrasonic. Additionally, Song et al. [9] studied the influence of ultrasonic power density, evaporation temperature and feed flow on the total energy consumption of ultrasonic evaporation. In terms of ultrasonic evaporation, the optimal conditions are as follows: ultrasonic power density is $4 \times 10^{-5} \text{ W/m}^2$, evaporation temperature is 65°C , and feed amount is $1.389 \times 10^{-5} \text{ m}^3/\text{s}$. Through orthogonal test and variance analysis, evaporation temperature has the greatest influence on total energy consumption, whereas ultrasonic power density has the least influence on total energy consumption. It is generally believed that by adding ultrasonics to the evaporation process, mass and heat can be transferred efficiently, increasing evaporation efficiency and reducing energy consumption.

The application of ultrasonic technology to the desalination process has been devoted to researchers both at home and abroad for strengthening the heat and mass transfer characteristics of ultrasonics. Banakar et al. [10] examined the influence of ultrasonic pretreatment on equipment scaling in seawater desalination. As a consequence, the solution was separated and filtered after testing revealed that the pretreatment had caused salt crystallisation. The solution was to be sent through the heat exchanger to investigate the effect of ultrasonic on the heat transfer rate of the solution. After analyzing the experimental data, the optimal parameters are determined as follows: under the conditions of ultrasonic frequency of 20 kHz, duty cycle of 50%, amplitude of 70% and irradiation for 30 min, the maximum heat transfer rate can reach 797 W/m^2 . Hosseingholilou et al. [11] evaluated the salinity and generated water volume of the ultrasonic desalination system by response surface methodology (RSM). In line with the findings, the salinity of the hot air dropped as its temperature rose; following the rise in ultrasonic power, the amount of water created increases. Optimal experimental variable values were derived by RSM for 1 h operation of the desalination system, which produced 200.737 mL of water with a salinity of 545 ppm. In addition, the economic analysis of the system proves that the operating cost and energy cost of the

system are less than those of the traditional RO and MSF methods. Zhang et al. [12] studied the response of seawater evaporation rate to temperature under different salinity. The results show that the ultrasonic evaporation speed increases with the increase of temperature. Resonance occurs when the inherent frequencies of ultrasonic and capillary waves in seawater are the same ones. Due to the evaporation speed that is accelerated by resonance, a suitable temperature for ultrasonic atomization is 50°C – 65°C .

This paper aims to investigate the effects of evaporation temperature, feed temperature, feed flow and ultrasonic power density of ultrasonic evaporator on performance ratio and specific heat transfer area of evaporator in the process of seawater desalination during single-effect evaporation. A single-effect evaporation seawater desalination system's performance may be improved theoretically and empirically using Minitab17 software.

2. Materials and experiments

2.1. Materials and equipments

2.1.1. Materials

The experiment is conducted with standard seawater in which the ratio of laboratory reagent to water is NaCl_2 6.518 g/L; MgSO_4 3.305 g/L; MgCl_2 2.447 g/L; CaCl_2 1.414 g/L; KCl 0.725 g/L; NaHCO_3 0.202 g/L. Total dissolved solids in seawater (TDS) approximately 35,000 ppm, pH 7.7–8.0.

2.1.2. Experimental equipments

It is an ultrasonic evaporator which was developed by our laboratory independently. The main instruments and equipment of the system is: central circulation tube evaporator, ultrasonic generator, ultrasonic transducer, condenser, vacuum pump and so on. Table 1 summarizes the characteristics of the ultrasonic evaporation system.

2.2. Experimental methods

2.2.1. Experimental steps

The flow chart of this experiment is illustrated in Fig. 1. To maintain the correct level of water in the tank for 6 and in the boiler for 7, fill it to two thirds of the level gauge. Pass seawater through the preheated tank 3, after heating to the set temperature, it is transmitted to the heating chamber at the lower end of ultrasonic evaporator 4 by feed pump 2. A portion of the seawater is supplied through the feed pipe, into the end of the evaporator by the way of the overflow from the bottom of the distributor, leaving the remainder as a liquid film in the inner wall of the evaporation tube, under the influence of the shell side steam temperature. The evaporated solution and the secondary steam enter the evaporation chamber, after separation, concentrated seawater enters the liquid storage tank 13 for measurement, and the secondary steam enters the condensate storage tank 11 for measurement after condensing through condenser 5.

A suitable evaporation temperature should first be determined, and then the input volume can be controlled by adjusting the rotameter. After the equipment runs

Table 1
Technical parameters

| Parameters | Evaporator shell side | Evaporator tube side |
|---------------------------------------------------|-----------------------|----------------------|
| Designing pressure (MPa) | 1.0 | –0.1 |
| Temperature (°C) | 100 | 100 |
| Operating pressure (MPa) | 0.1–0.5 | –0.08–0.3 |
| Operating temperature (°C) | 60–100 | 40–125 |
| Medium | 110°C saturated steam | 35,000 ppm seawater |
| Weld joint coefficient | 0.85 | 0.85 |
| Corrosion margin (mm) | 1.0 | 1.0 |
| Insulation material thickness (mm) | 30 | – |
| Ultrasonic generator power (W) | 0–1,000 | – |
| Ultrasonic transducer (W) | 0–1,200 | – |
| Material of main pressure components | 06Cr19Ni10 | – |
| Volume of ultrasonic evaporator (m ³) | 0.125 | – |
| Diameter of evaporation tube (mm) | – | φ20 × 2.5 |
| Length of evaporation tube (m) | – | 0.5 |
| Pressure in the boiler (MPa) | 0.1–0.3 | – |
| Power of electric heating furnace (kW) | 9 | – |

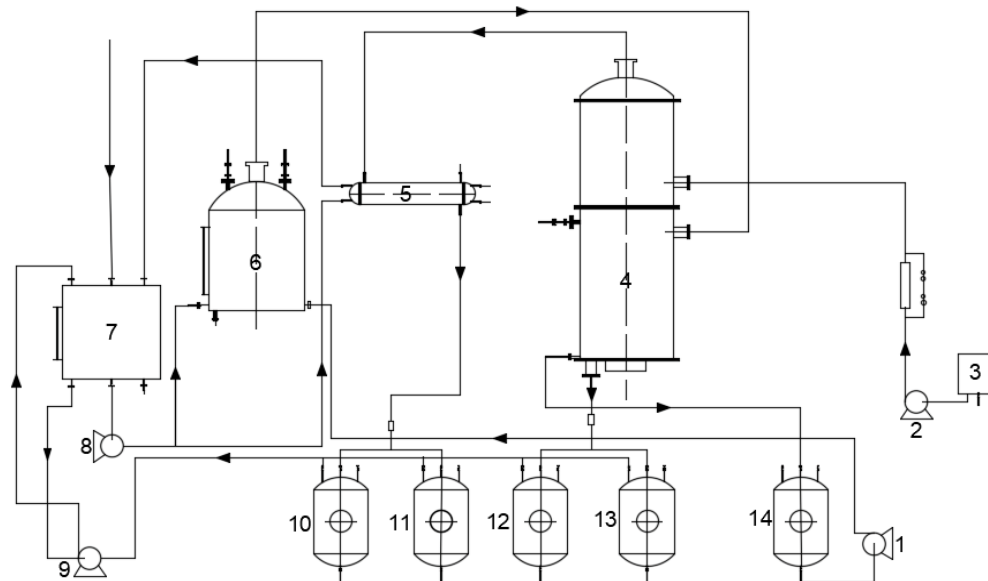


Fig. 1. Ultrasonic evaporator device process graph. 1. Circulating pump, 2. Input pump, 3. Preheating tank, 4. Ultrasonic evaporator, 5. Condenser, 6. Boiler, 7. Water tank, 8. Pipeline pressure booster pump, 9. Vacuum pump, 10, 11, 14. Condensate storage tank, 12, 13. Complete liquid storage tank.

smoothly, turn on the ultrasonic generator and adjust it to the certain value, observe the discharge of concentrated salt water and fresh water, start timing after it is stable, measure and record the amount of fresh water and raw steam condensate every 10 min.

2.2.2. Calculation of performance ratio and specific heat exchange area of evaporator

A reliable measurement is made by repeating three experiments on each group of data, and the median is taken

as the measure. Performance ratio, PR is the amount of fresh water produced by heating steam per unit, which can be used to measure the operating cost of the system. Increase of performance ratio can effectively reduce the energy consumption of the system; specific heat transfer area of evaporator, the sA_e is the effective heat exchange area provided by the evaporator when producing distilled water per unit mass flow, reducing specific heat transfer area of evaporator can effectively reduce the investment cost of the system. As a function of the performance ratio and the specific area of heat transfer, it is as follows:

$$PR = \frac{M_d}{M_s} \tag{1}$$

$$sA_e = \frac{A_e}{M_d} \tag{2}$$

where M_d refers to the flow of distilled water, kg/h; M_s is heating steam mass flow, kg/h; A_e is the effective heat transfer area of the evaporator, m².

2.2.3. Design of the single factor experiment

According to the data in references and pre-experimental analysis, the evaporation temperature (70°C, 75°C, 80°C, 85°C, and 90°C), feed temperature (45°C, 55°C, 65°C, 75°C, and 85°C), input temperature (25, 35, 45, 55, and 65 kg/h) and the influence of ultrasonic power density (0, 0.4, 0.6, 0.8, 1.0, and 1.2 W/cm²) on performance ratio and specific heat transfer area of evaporator. Through pre-experimental research, the initial conditions for single-factor experiments are set as: evaporation temperature 80°C, input temperature 65°C, input flow 45 kg/h, ultrasonic power density are 0 and 0.8 W/cm².

2.2.4. Design of the response surface experiment

According to the Box–Behnken experimental design, we use Minitab17, take the evaporation temperature (X_1 /°C), the input temperature (X_2 /°C), the input flow (X_3 /(kg/h)), the ultrasonic power density (X_4 /(W/cm²)) as main factors to carry out an experiment examining 4 factors in three levels, so as to increase performance ratio. The levels and codes of each factor are shown in Table 2.

3. Results and discussion

3.1. Analysis of the single factor experiment

3.1.1. Influence of evaporation temperature on performance ratio of the evaporator

The impact of evaporation temperature when there is no ultrasonic power density compared to ultrasonic power density of 0.8 W/cm² on performance ratio and specific heat transfer area of the evaporator was studied. The input temperature was 65°C and the input flow was 45 kg/h. The experimental results are shown in Figs. 2 and 3.

From Fig. 2 that the gained output ratio of the system increases with the increase of the evaporation temperature,

which is slow when the evaporation temperature exceeds 80°C. A system which provides evaporation at 70°C–90°C will improve its performance ratio by 7.26%–11.81% with ultrasonics added. As the evaporation temperature increases, the viscosity of seawater gradually decreases, the residence

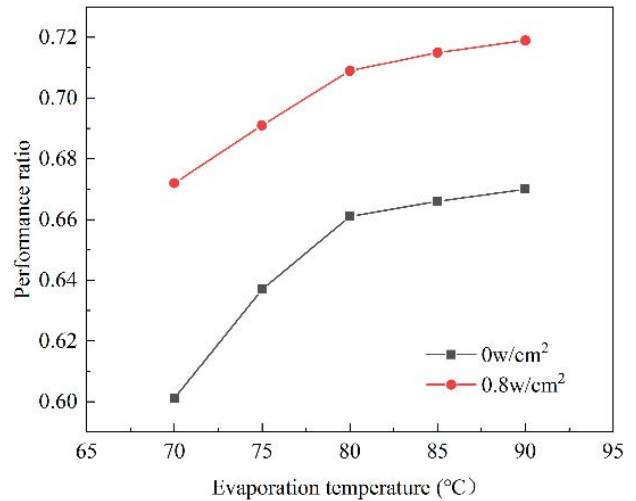


Fig. 2. Effect of evaporation temperature on performance ratio.

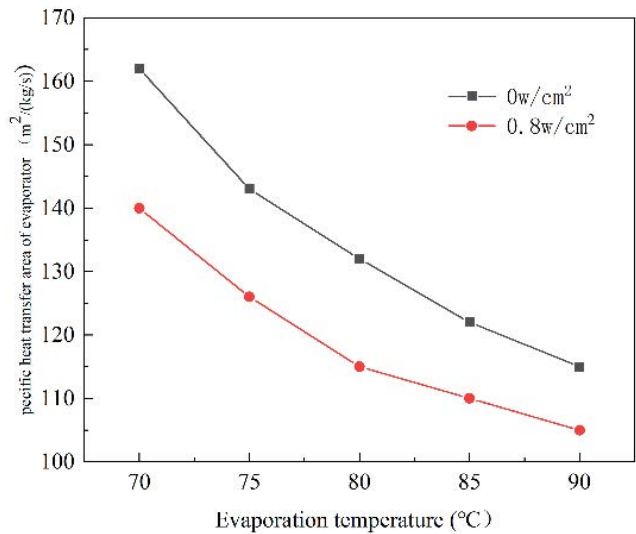


Fig. 3. Effect of evaporation temperature on specific heat transfer area of evaporator.

Table 2 Performance ratio response surface test design table

| Levels | | Factors | | | |
|--------|------------------------------------|------------------------------|-------------------------|-----------------------------------------------------|--|
| | X_1 evaporation temperature (°C) | X_2 input temperature (°C) | X_3 input flow (kg/h) | X_4 ultrasonic power density (W/cm ²) | |
| -1 | 75 | 65 | 35 | 0.8 | |
| 0 | 80 | 75 | 45 | 1.0 | |
| 1 | 85 | 85 | 55 | 1.2 | |

time of the liquid film in the heat exchange tube becomes shorter, the thickness becomes smaller, and the heat transfer resistance is reduced, thereby enhancing heat transfer and increasing the water production ratio of the equipment. Since there is no evident improvement of performance ratio and considerable rise in energy consumption, after comprehensively considering, 80°C is the best evaporation temperature for performance ratio (namely performance ratio). The final ratio is 0.709.

Fig. 3 shows that specific heat exchange area of the evaporator decreases with the increase of the evaporation temperature. When the evaporation temperature exceeds 85°C, the decrease rate tends to be flatter. When an ultrasonic wave is combined with evaporation temperature 70–90°C, specific heat transfer area of evaporator decreases by 8.7%–13.58%. Boosting the evaporation temperature will increase the degree of turbulence and increase the liquid vaporization volume and vaporization speed, consequently increasing the evaporation rate and increasing the water production per evaporation area. As a result, the specific heat exchange area decreases as the evaporation temperature rises. The equipment's running expenses are proportional to the equipment's specific heat exchange area. In light of the aforementioned considerations, 85°C is chosen as the optimal evaporation temperature for the evaporator's specific heat exchange area. At this time, specific heat exchange area of the evaporator is 110 m²/(kg/s).

3.1.2. Influence of the feed temperature on performance ratio of the evaporator

When the evaporation temperature is 80°C and the feed flow is 45 kg/h, we compare the impact of feed temperature on performance ratio and specific heat transfer area of evaporator when there is no ultrasonic power density against the ultrasonic power density of 0.8 W/cm². Figs. 4 and 5 illustrate the final outcome.

It can be observed in Fig. 4 that the system performance ratio increases with the increase of the feed temperature,

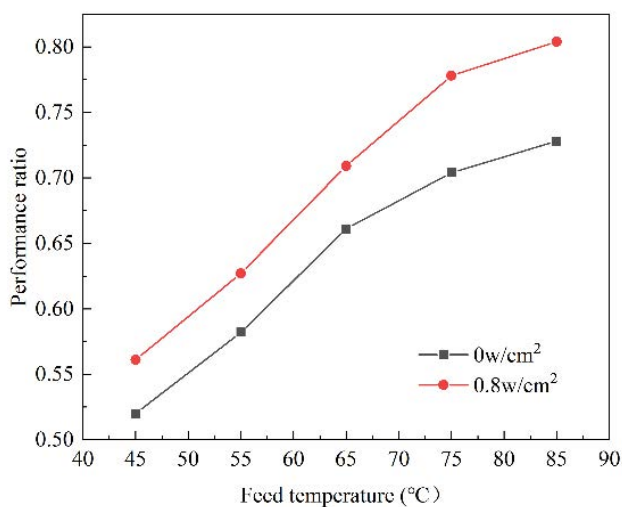


Fig. 4. Effect of feed temperature on performance ratio.

but when the feed temperature is greater than 75°C, the increase in the water production ratio tends to be flat. When the feed temperature is 45°C–85°C, performance ratio of the system increases by 7.31%–10.51%. When the feed temperature is 45°C–75°C, as the temperature increases, the quantity of steam required for the preheating process decreases, and the specific gravity of the heated steam used to evaporate seawater increases. Because of this, evaporation efficiency is substantially increased, and the performance ratio improves quicker, since the nucleate boiling of the liquid film happens on the heat exchange tube's inner wall.; when the feed temperature is greater than 75°C, more bubbles gather on the surface of the liquid film, the nucleate boiling gradually changes to the film boiling, the thermal resistance on the wall of the heat exchange tube becomes larger, and the heat transfer of the liquid film is restricted, resulting in a slowly increase in performance ratio. For seawater desalination, there is no significant increase in performance ratios at 75°C–85°C, and the higher temperature will result in wasted energy. Based on the information presented above, 75°C would be an appropriate choice at the test center at this time, with an overall performance ratio of 0.778.

From Fig. 5 it is apparent that the specific heat transfer area of an evaporator decreases with an increasing feed temperature. As the feed temperature exceeds 75°C, specific heat transfer areas of evaporator decrease slowly; a constant decrease in feed temperature leads to a decreasing specific heat exchange area in an evaporator. A comparison of the specific heat transfer area in an evaporator with and without ultrasonic evaporation showed that when feed temperatures drop to 45°C–85°C via ultrasonic action, the specific heat transfer area decreases to 9.32%–17.01%. The sensible heat consumption of the evaporator decreases with increasing feed temperature, the heat flux increases, and the evaporation intensity rises, thereby reducing seawater viscosity. Therefore, the flow of seawater on the wall surface is promoted, so as to strengthen the heat transfer and effectively minimize specific heat transfer area of the evaporator.

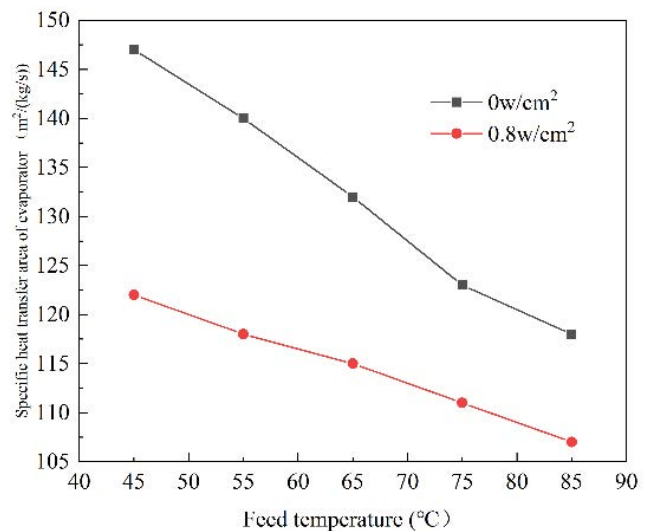


Fig. 5. Effect of feed temperature on specific heat transfer area of evaporator.

Based on the above factors, the optimal feed temperature of specific heat transfer area of evaporator is selected as 75°C, and specific heat transfer area of the evaporator is 111 m²/(kg/s) currently.

3.1.3. Influence of the feed flow on performance ratio of the evaporator

When the evaporation temperature is 80°C and the feed temperature is 65°C, the influence of the change of feed flow on performance ratio and specific heat transfer area of evaporator without ultrasonic and the ultrasonic power density is 0.8 W/m². The experimental results are shown in Figs. 6 and 7.

It is apparent from Fig. 6 that the water generation ratio slowly increases with increasing feed flow. In feed flow

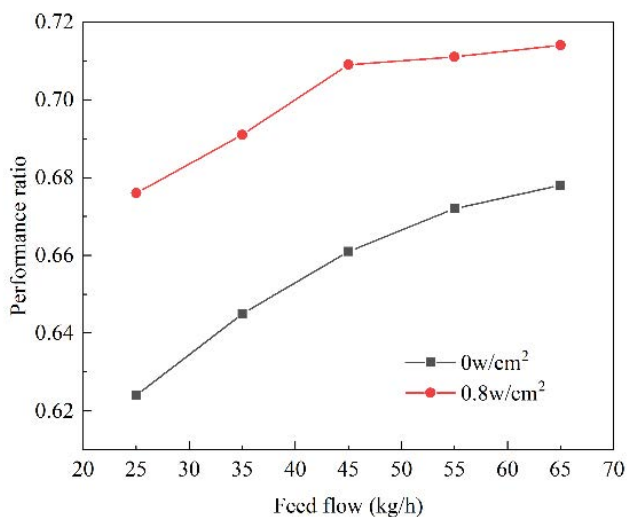


Fig. 6. Effect of feed flow on performance ratio.

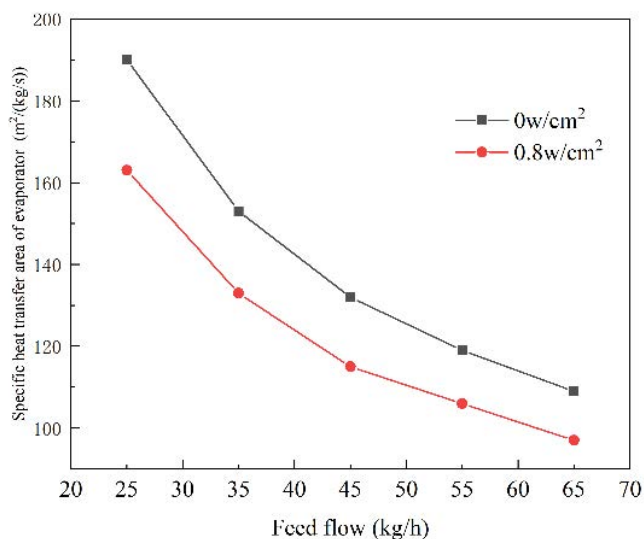


Fig. 7. Effect of feed flow on specific heat transfer area of evaporator.

range of 25–65 kg/h, compared with the experiment without ultrasound, performance ratio increased by 5.31%–8.33% with the addition of ultrasound. The feed flow of seawater becomes larger, the circulation speed of seawater in the evaporator accelerates, and the degree of turbulence increases; an increase in evaporation rate is achieved by increasing the heat transfer area of the liquid layer on the heat exchange surface. With ultrasound, if the seawater input flow is less than 45 kg/h, the heat exchange area of the evaporator is completely exploited, and the performance ratio will grow quicker; At feed rates more than 45 kg/h, the seawater's duration in the heat exchange tube is reduced, sensible heat is used more quickly, external steam is used more readily, and the upward trend in the performance ratio is halted. Taking into account all of the aforementioned considerations, it is appropriate to pick a feed flow of 45 kg/h and a performance ratio of 0.709 at this moment.

It can be seen from Fig. 7 that when the feed flow increases, the evaporator specific heat transfer area of evaporator decreases and the downward trend is not visible when it is greater than 55 kg/h. In the range of 25–65 kg/h of feed flow, specific heat transfer area of evaporator decreases by 11.01%–14.21% after adding ultrasonic. As the feed flow increases, the renewal speed of the liquid film in the heat exchange tube of the evaporator at a quicker rate, and the degree of turbulence increases. The entire surface area for heat exchange in the evaporator stays constant. In proportion to the heat transfer efficiency and the amount of secondary steam increase, the required evaporation area per unit mass flow decreases. In light of the above factors, it is best when the feed flow of specific heat transfer area of evaporator is 55 kg/h, at this time specific heat transfer area of evaporator is 106 m²/(kg/s).

3.1.4. Influence of ultrasonic power density on performance ratio of the evaporator

When the evaporation temperature is 80°C, the feed temperature is 65°C, and the feed flow is 45 kg/h, the changing trend of seawater desalination performance ratio and specific heat transfer area of evaporator under various ultrasonic power densities is discussed. The experimental results are shown in Figs. 8 and 9.

It can be seen from Fig. 8 that when the ultrasonic power density of the evaporator is in the interval of 0–1.0 W/cm², performance ratio is positively correlated with it; when it comes to performance ratio, a negative correlation exists in the range of 1.0–1.2 W/cm². At a power density of 1.0 W/cm², the performance ratio achieves its highest value of 0.719%. Cavitation bubbles are created when high pressure and high temperature are produced as a result of the instantaneous shock waves generated by the ultrasonic waves acting on liquid film. The cavitation bubbles burst and cause high temperatures and pressures to occur, atomizing the seawater nearby to reach nucleate boiling. The field's interior has been totally heated and swapped. Internal fluid circulation speed and energy exchange rate increase when the cavitation bubbles exit from heat exchanger walls, resulting in an increase in overall efficiency. It is unable to break the cavitation bubbles at 1.0 W/cm² ultrasonic power

density, therefore the vaporisation in the heat exchange tube is lowered and the heat transmission is hindered.

It can be seen from Fig. 9 that when the ultrasonic power density is in the range of 0–1.0 W/cm², specific heat transfer area of evaporator decreases with its increase; in the range of 1.0–1.2 W/cm², specific heat transfer area of evaporator increases with its increase. When the ultrasonic power density is 1.0 W/cm², specific heat exchange area of the evaporator attains the minimum value of 113 m²/(kg/s). It becomes more difficult for cavitation bubbles to form in the evaporator tube due to an increase in ultrasonic power density. This causes the boundary layer of the tube to become more disturbed, increasing heat exchange efficiency while decreasing specific heat exchange area. At ultrasonic power densities exceeding 1.0 W/cm², the cavitation bubbles in the tube do not have sufficient time to burst, resulting in a decrease in the vaporization efficiency of the fluid. Inhibition of heat transfer increases specific heat exchange area.

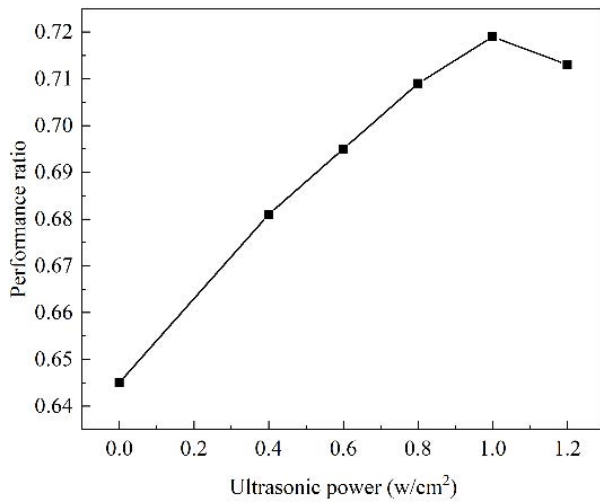


Fig. 8. Effect of ultrasonic power density on performance ratio.

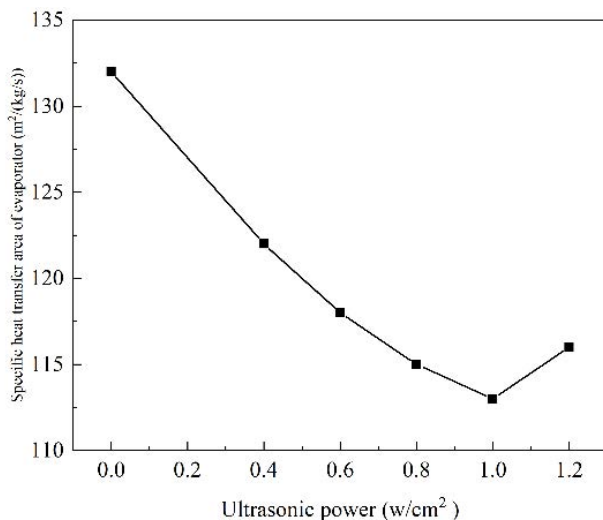


Fig. 9. Effect of ultrasonic power density on specific heat transfer area of evaporator.

3.2. Response surface test analysis

3.2.1. Model establishment and significance test

The goal of this study is to determine the performance ratio of the evaporator using the following parameters: evaporation temperature, feed temperature, feed flow rate, ultrasonic power density. The Box–Behnken test design scheme and outcomes are listed in Table 3. The whole test has a total of 27 groups, of which the center point test is repeated in 3 groups.

Use Minitab17 software to fit performance ratio in Table 3 to obtain the regression equation: $Y = -5.04 + 0.1021X_1 + 0.0201X_2 + 0.00903X_3 + 1.07X_4 - 0.000632X_1X_1 - 0.000113X_2X_2 - 0.000123X_3X_3 - 0.5448X_4X_4 + 0.000045X_2X_3$. Among them, X_1X_1 , X_2X_2 , X_3X_3 , X_4X_4 represent the square term, and X_2X_3 is the interactive term. For each component, the main and secondary order of importance is as follows: ultrasonic power density > evaporation temperature > feed temperature > feed flow. The aforementioned regression equation was subjected to an analysis of variance, the results of which are shown in Table 4.

It can be seen from Table 4 that the established model has a high F -value ($F = 205.29$) and a very low P -value ($P < 0.001$), indicating that the quadratic equation model is noteworthy; The lack of fit item $P > 0.05$ is not statistically significant, showing that non-test variables have minimal influence on test outcomes, hence the model's dependability is excellent. The significance test for the analysis of variance reveals that the four parameters of evaporation temperature, feed temperature, feed flow, and ultrasonic power density have a significant effect on the inspection indicators. It can be seen from the results that the correlation coefficient R^2 of the model is 99.09%, and the adjusted R^2 is 98.61%, indicating that there is a significant linear relationship between performance ratio and independent variables with good fitting degree, and the correlation of the independent variables in determining performance ratio is significant.

The A-D normality test of performance ratio shows that the P -value = 0.787 > 0.05, indicating that performance ratio conforms to the normal distribution. X_1 , X_2 , X_3 and Y all showed Pearson correlation coefficients of 0.087, 0.917, and 0.237, which indicated a positive linear correlation between each group of variables. X_4 and Y have a Pearson correlation coefficient of -0.069 , implying a positive linear relationship. The error between the predicted value and the actual value is lower than 0.01 in each group.

3.2.2. Response surface analysis

The contour map (two-dimensional) and the surface map (three-dimensional) of the model are presented in Figs. 10–15. As such, they intuitively influence the performance ratio as a result of a two-way interaction. The slope of the curved surface determines the significance of the interaction effect of the curved surface on the water production ratio. In an evaporator, when the surface slope and the evaporation rate change slightly, the evaporation ratio will become more sensitive to changes in surface slope.

Fig. 10 shows the contour plot of the evaporating temperature with respect to the performance ratio in addition to a surface plot of the feed temperature. As depicted

Table 3
Response surface analysis scheme and test results of water production ratio

| Number | X_1 evaporation temperature (°C) | X_2 input temperature (°C) | X_3 input flow (kg/h) | X_4 ultrasonic power density (W/cm ²) | Y performance ratio |
|--------|------------------------------------|------------------------------|-------------------------|-----------------------------------------------------|---------------------|
| 1 | 75 | 65 | 45 | 1.0 | 0.697 |
| 2 | 85 | 65 | 45 | 1.0 | 0.719 |
| 3 | 75 | 85 | 45 | 1.0 | 0.809 |
| 4 | 85 | 85 | 45 | 1.0 | 0.818 |
| 5 | 80 | 75 | 35 | 0.8 | 0.745 |
| 6 | 80 | 75 | 55 | 0.8 | 0.768 |
| 7 | 80 | 75 | 35 | 1.2 | 0.737 |
| 8 | 80 | 75 | 55 | 1.2 | 0.765 |
| 9 | 75 | 75 | 45 | 0.8 | 0.756 |
| 10 | 85 | 75 | 45 | 0.8 | 0.762 |
| 11 | 75 | 75 | 45 | 1.2 | 0.740 |
| 12 | 85 | 75 | 45 | 1.2 | 0.748 |
| 13 | 80 | 65 | 35 | 1.0 | 0.705 |
| 14 | 80 | 85 | 35 | 1.0 | 0.804 |
| 15 | 80 | 65 | 55 | 1.0 | 0.718 |
| 16 | 80 | 85 | 55 | 1.0 | 0.835 |
| 17 | 75 | 75 | 35 | 1.0 | 0.739 |
| 18 | 85 | 75 | 35 | 1.0 | 0.746 |
| 19 | 75 | 75 | 55 | 1.0 | 0.772 |
| 20 | 85 | 75 | 55 | 1.0 | 0.779 |
| 21 | 80 | 65 | 45 | 0.8 | 0.709 |
| 22 | 80 | 85 | 45 | 0.8 | 0.802 |
| 23 | 80 | 65 | 45 | 1.2 | 0.701 |
| 24 | 80 | 85 | 45 | 1.2 | 0.804 |
| 25 | 80 | 75 | 45 | 1.0 | 0.785 |
| 26 | 80 | 75 | 45 | 1.0 | 0.789 |
| 27 | 80 | 75 | 45 | 1.0 | 0.790 |

Table 4
Analysis of variance of response surface test results

| Source | Degree of freedom | Adj. SS | Adj. MS | F-value | P-value |
|-------------|-------------------|----------|----------|---------|---------|
| Return | 9 | 0.038094 | 0.004233 | 205.29 | 0.000 |
| X_1 | 1 | 0.001355 | 0.001355 | 65.74 | 0.000 |
| X_2 | 1 | 0.000854 | 0.000854 | 41.42 | 0.000 |
| X_3 | 1 | 0.000278 | 0.000278 | 13.48 | 0.002 |
| X_4 | 1 | 0.002432 | 0.002432 | 117.94 | 0.000 |
| X_1X_1 | 1 | 0.001330 | 0.001330 | 64.51 | 0.000 |
| X_2X_2 | 1 | 0.000680 | 0.000680 | 32.98 | 0.000 |
| X_3X_3 | 1 | 0.000806 | 0.000806 | 39.08 | 0.000 |
| X_4X_4 | 1 | 0.002533 | 0.002533 | 122.84 | 0.000 |
| X_2X_3 | 1 | 0.000081 | 0.000081 | 3.93 | 0.064 |
| Error | 17 | 0.000351 | 0.000021 | – | – |
| Lack of fit | 15 | 0.000336 | 0.000022 | 3.20 | 0.263 |
| Pure error | 2 | 0.000014 | 0.000007 | – | – |
| Total | 26 | 0.038444 | – | – | – |

in Fig. 10a, the performance ratio increases progressively with increasing feed temperature while keeping the evaporation temperature constant; in the presence of constant feed temperatures, the performance ratio increases and then decreases with increasing evaporation temperature, but no clear trend can be discerned. With an increase in feed temperature around 65°C~75°C, the contour line becomes denser, which indicates that the performance ratio is increasing significantly. Fig. 10b shows that modifying only the evaporation temperature and the feed temperature influences the performance ratio to a greater extent.

Fig. 11 displays a contour plot and a curved surface plot of the evaporation temperature and the feed flow with respect to the water production ratio. At the centre level, the elliptical contour lines are seen in Fig. 11a. Temperature and feed flow rate do not interact much in the evaporation process. As input flow increases, the performance ratio eventually approaches its maximum value, regardless of the evaporation temperature; when the feed flow remains constant, performance ratio first increases and subsequently declines as the increase of the evaporation temperature. The optimal evaporation temperature and feed flow are between 79.0°C and 82.5°C and 46.5 and 54.5 kg/h,

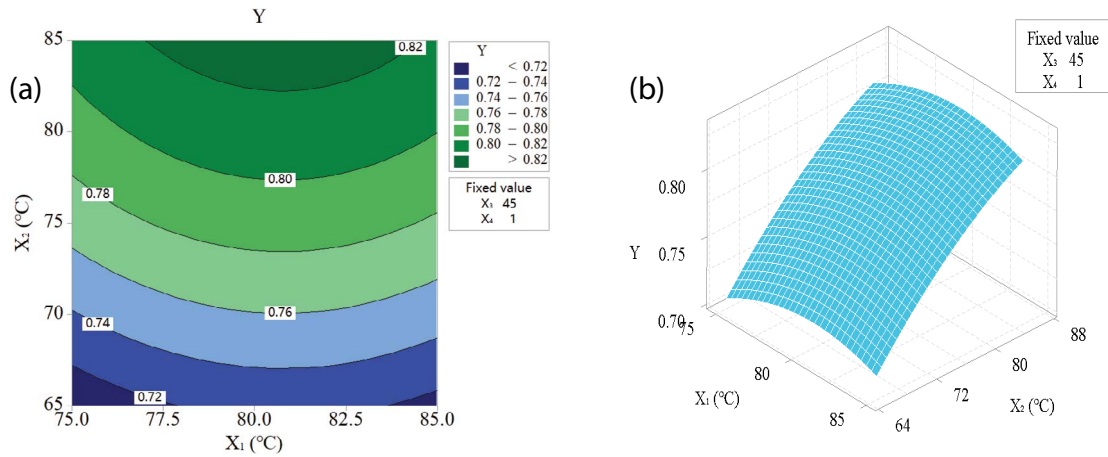


Fig. 10. Contour map and surface graph of performance ratio and evaporation temperature and feed temperature.

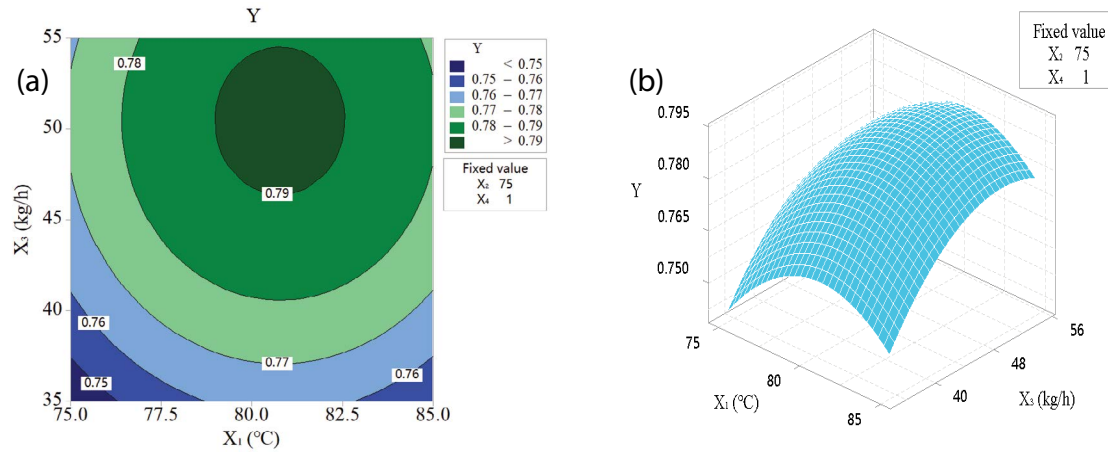


Fig. 11. Contour map and surface graph of performance ratio and evaporation temperature and feed flow.

respectively. Fig. 11b shows that when only the evaporation temperature and the feed flow are altered, the change of the feed flow has a more significant impact on performance ratio, and the response surface is convex, indicating that there is a maximum value under the interaction between the evaporation temperature and the feed flow. When the evaporation temperature is 80.7°C and the feed flow is 50.5 kg/h, performance ratio sets the maximum value of 0.792.

Fig. 12 depicts the contour plot and surface plot of evaporation temperature, ultrasonic power density and performance ratio. Fig. 12a shows oval contour lines for evaporation temperature and ultrasonic power density, indicating no substantial interaction between the two variables. As just the ultrasonic power density is raised without changing the evaporation temperature, performance ratio increases first and then decreases; the performance ratio increases to its maximum and then decreases slightly as the evaporation temperature increases with constant ultrasonic power density. In the range of 77.1°C × 84.5°C, the evaporation temperature is higher, and the ultrasonic power density is greater (1.106 W/cm²), so the performance

ratio is greater. The response surface in Fig. 12b is convex, giving an indication of the interaction between evaporation temperature and ultrasonic power density is under a maximum value. A maximum performance ratio of 0.789 results from an evaporation temperature of 80.7°C and an ultrasonic power density of 0.987 W/cm².

As shown in Fig. 13, the feed temperature, feed flow, and performance ratio are depicted as contour plots and curved surface plots respectively. In Fig. 13a, the performance ratio significantly increases with increasing feed temperature, as long as the feed flow remains constant; The performance ratio initially increases with an increase in feed flow, but then tends to remain flat as the feed temperature remains constant. The regression model indicated that the relationship between feed temperature and feed flow had an important effect on performance ratios when they interact during the evaporation process. At 65°C–75°C of feed temperature, the contour line is denser. At this time, the performance ratio rises dramatically as feed temperature is raised. Fig. 13b demonstrates that feed temperature has a greater impact on the performance ratio when only feed temperature and feed flow are changed.

An illustration of the contour plot and the curved surface plot of feed temperature and ultrasonic power density based on performance ratio is provided in Fig. 14. Fig. 14a illustrates how as the ultrasonic power density increases,

the performance ratio initially increases and then decreases while keeping the feed temperature constant; with an increase in temperature along with a constant ultrasonic power density, the increase in generation ratio suffers

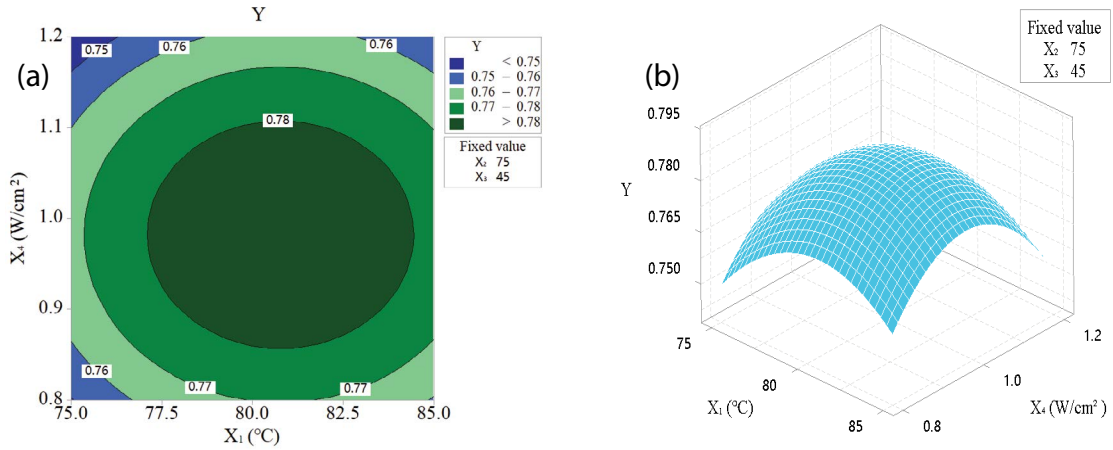


Fig. 12. Contour map and surface graph of performance ratio and evaporation temperature and ultrasonic power density.

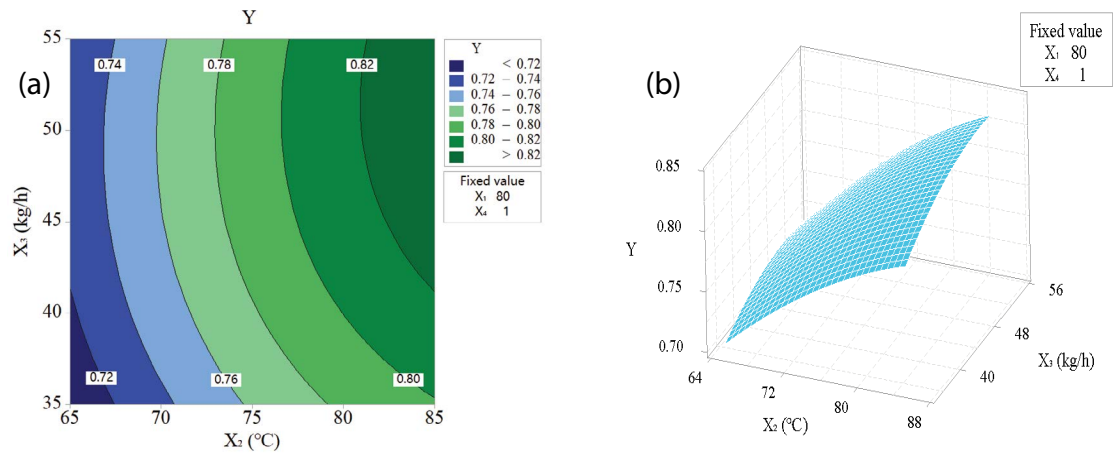


Fig. 13. Contour map and surface graph of performance ratio and feed temperature and feed flow.

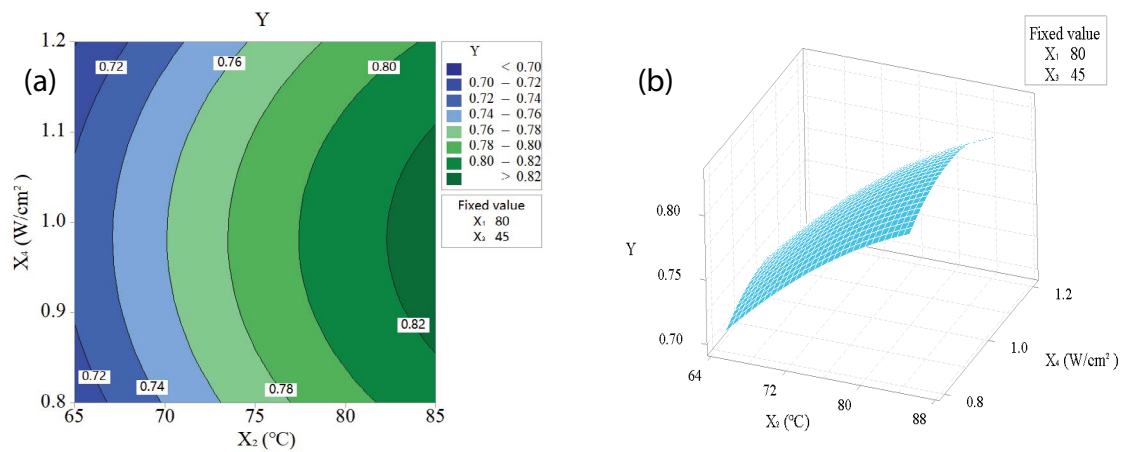


Fig. 14. Contour map and surface graph of performance ratio and feed temperature and ultrasonic power density.

from a gradual slowdown as the contour line becomes sparse. When the ultrasonic power density is constant, the increase in generation ratio gradually becomes slower as the contour line changes from dense to sparse with increase in feed temperature. It can be seen from Fig. 14b that when only the temperature of the feed and the density of the ultrasound power are changed, the temperature of the feed has a greater impact on the performance ratio, while the density of ultrasound power has no notable impact on the performance ratio. In Fig. 14b the affect of feed temperature and ultrasound power density on performance ratio are shown to be more significant when they are changed individually, as the feed temperature has a more significant impact than the ultrasound power density.

Fig. 15 illustrates the contour plot and surface plot of the feed flow, ultrasonic power density and performance ratio. Fig. 15a, where the contour lines of feed flow and ultrasonic power density are oval, shows that there is no significant interaction between these two parameters in affecting the performance ratio. In a continuous flow system and only the power density of ultrasonic waves is increased, the performance ratio increases at first and then decreases; as

the ultrasonic power density is constant, the water generation ratio will increase as the feed flow increases, reaching its maximum before flattening out. When the feed flow is 46.6–54.3 kg/h and the ultrasonic power density is within the range of 0.926–1.038 W/cm², performance ratio can achieve the maximum value. A convex response surface is illustrated in Fig. 15b whereby there is an interaction between feed flow and ultrasonic power density that results in a maximum value. When the feed flow is 50.4 kg/h and the ultrasonic power density is 0.984 W/cm², performance ratio is achieved the maximum value is 0.792.

3.2.3. Optimal process conditions prediction and verification

Fig. 16 demonstrates how to optimise the resulting regression equation using Minitab 17 and a confidence interval of 95%. The experimental results indicate that the optimum operating conditions influence performance ratio: evaporation temperature 80.76°C, feed temperature 85°C, feed flow 52.37 kg/h, ultrasonic power density 0.98 W/cm². At this time, performance ratio reaches the maximum value of 0.836. Evaporation temperature 80°C, feed temperature

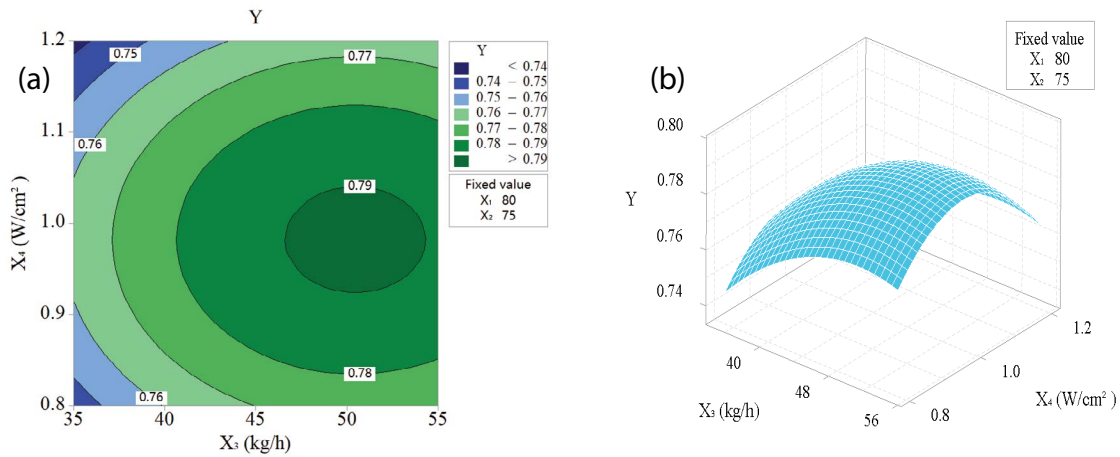


Fig. 15. Contour map and surface graph of performance ratio and feed flow and ultrasonic power density.

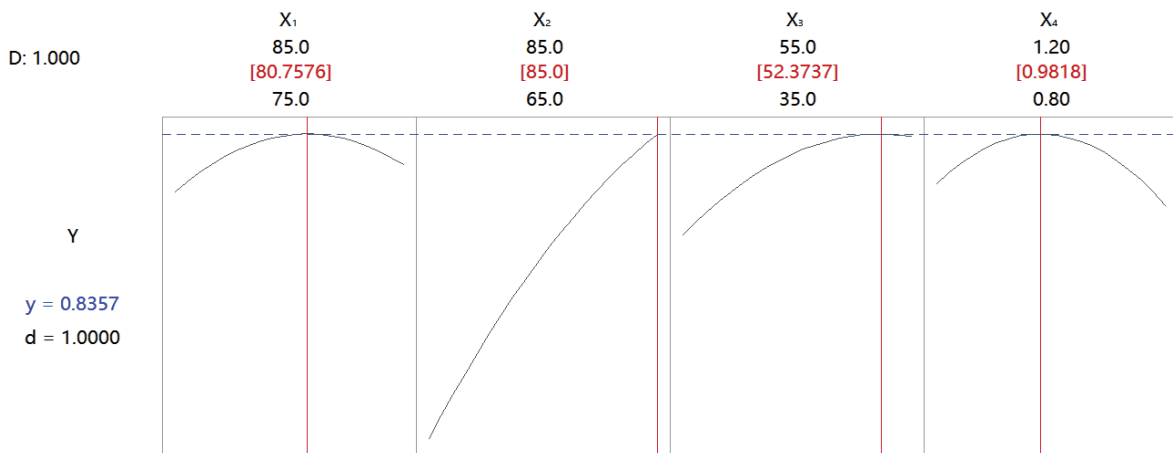


Fig. 16. Optimal diagram of performance ratio.

85°C, feed flow 50 kg/h, ultrasonic power density 1.0 W/cm² were changed as the ideal process parameters to simplify the real operation. Under this optimal condition, the experiment was repeated three times to eliminate the error, and performance ratio of the evaporator was obtained as 0.832, which was consistent with the anticipated value of the model (0.836), indicating that the response surface model can perform a better performance ratio situation of the evaporator prediction.

4. Conclusion

For the purpose of solving the problems of insufficient heat transfer and low evaporation efficiency in the process of seawater desalination by traditional distillation, our laboratory independently developed a set of central circulation tube evaporator that can be added with ultrasonic, and applied it in the process of seawater desalination. With the help of a response surface test combined with a single factor, the effects of evaporation temperature, feed temperature, feed flow rate, and ultrasonic power density on performance ratio and specific heat transfer area of evaporators were examined, and the ratio of performance was optimized, providing a mathematical model and data support for improving seawater desalination efficiency.

Under the individual action of each component, inclusion of 0.8 W/cm² ultrasonic waves can increase performance ratio of the evaporator by 5.31%–11.81% and reduce specific heat transfer area of the evaporator by 8.7%–17.01%. An analysis of 4 factors and 3 levels of the distillation seawater desalination process parameters was performed. As follows: ultrasonic power density > evaporation temperature > feed temperature > feed flow rate significantly influenced the performance ratio. The regression equation of evaporation temperature (X_1), feed temperature (X_2), feed flow rate (X_3), ultrasonic power density (X_4) and evaporator water production ratio (Y) is: $Y = -5.04 + 0.1021X_1 + 0.0201X_2 + 0.00903X_3 + 1.07X_4 - 0.000632X_1X_1 - 0.000113X_2X_2 - 0.000123X_3X_3 - 0.5448X_4X_4 + 0.000045X_2X_3$. Analyzing the maximum model and verifying experimentally provide the results: maximum evaporation performance ratio of 0.832 can be achieved over an evaporation temperature of 80°C, a feed temperature of 85°C, a feed flow of 50 kg/h, and an ultrasonic power density of 1.0 W/cm².

Acknowledgement

The research reported herein was funded by the Tianjin Graduate Scientific Research Innovation Project

for funding this work (Project No. 2020YJSS058). Thanks again for the financial support (Tianjin Graduate Scientific Research Innovation Project).

The opinions and findings expressed in this research are only those of the authors.

References

- [1] S. Dangwal, R.C. Liu, L.D. Bastatas, E. Echeverria, C.Q. Huang, Y. Mao, D.N. McIlroy, S. Han, S.-J. Kim, ZnO microfiltration membranes for desalination by a vacuum flow-through evaporation method, *Membranes*, 9 (2019) 156, doi: 10.3390/membranes9120156.
- [2] E.M.S. El-Said, M.A. Dahab, M. Omara, G.B. Abdelaziz, Solar desalination unit coupled with a novel humidifier, *Renewable Energy*, 180 (2021) 297–312.
- [3] S.Y. Liu, Z.Y. Wang, M.Y. Han, G.D. Wang, T. Hayat, G.Q. Chen, Energy-water nexus in seawater desalination project: a typical water production system in China, *J. Cleaner Prod.*, 279 (2021) 123412, doi: 10.1016/j.jclepro.2020.123412.
- [4] L. Mathieu, G. Nicolas, L.P. Stéphane, B. Primius, B. André, B. Mostafa, Enhancement of heat transfer by ultrasound: review and recent advances, *Int. J. Chem. Eng.*, 2021 (2011) 670108, doi: 10.1155/2011/670108.
- [5] V.I. Trushlyakov, I.Y. Lesnyak, A.A. Novikov, Impact of ultrasonic exposure and external pressure in a closed volume on the temperature of the evaporated liquid, *J. Phys. Conf. Ser.*, 1441 (2020) 012120, doi: 10.1088/1742-6596/1441/1/012120.
- [6] M.M. Ghafurian, Z. Akbari, H. Niazmand, R. Mehrkhah, S. Wongwises, O. Mahian, Effect of sonication time on the evaporation rate of seawater containing a nanocomposite, *Ultrason. Sonochem.*, 61 (2020) 104817, doi: 10.1016/j.ultsonch.2019.104817.
- [7] M. Dehbani, M. Rahimi, Introducing ultrasonic falling film evaporator for moderate temperature evaporation enhancement, *Ultrason. Sonochem.*, 42 (2018) 689–696.
- [8] J.T. Song, Y.X. Feng, W. Tian, J.B. Liu, Y.N. Wang, X.F. Xu, Enhancement of heat transfer performance using ultrasonic evaporation, *Int. J. Food Eng.*, 15 (2019) 20180337, doi: 10.1515/ijfe-2018-0337.
- [9] J.T. Song, H. Su, W. Tian, Y.X. Feng, W.C. Wang, Energy consumption evaluation of liquid food ultrasonic evaporation process, *Int. J. Food Eng.*, 16 (2020) 20190320, doi: 10.1515/ijfe-2020-0007.
- [10] V.V. Banakar, S.S. Sabnis, P.R. Gogate, A. Raha, Saurabh, Improvements in heat transfer in thermal desalination operation based on removal of salts using ultrasound pretreatment, *Ultrason. Sonochem.*, 69 (2020) 105251, doi: 10.1016/j.ultsonch.2020.105251.
- [11] B. Hosseingholilou, A. Banakar, M. Mostafaei, Design and evaluation of a novel ultrasonic desalination system by response surface methodology, *Desal. Water Treat.*, 164 (2019) 263–275.
- [12] L. Zhang, H. Dong, X. Wang, Temperature Response in the Process of Ultrasonic Seawater Desalination, 2011 Asia-Pacific Power and Energy Engineering Conference, IEEE, Wuhan, China, 2011, pp. 1–4, doi: 10.1109/APPEEC.2011.5748641.